

Invited Paper

# The CAOS Camera Platform – Ushering in a Paradigm Change in Extreme Dynamic Range Imager Design

Nabeel A. Riza

School of Engineering, University College Cork

College Road, Cork, Ireland

Email: n.riza@ucc.ie

## ABSTRACT

Multi-pixel imaging devices such as CCD, CMOS and Focal Plane Array (FPA) photo-sensors dominate the imaging world. These Photo-Detector Array (PDA) devices certainly have their merits including increasingly high pixel counts and shrinking pixel sizes, nevertheless, they are also being hampered by limitations in instantaneous dynamic range, inter-pixel crosstalk, quantum full well capacity, signal-to-noise ratio, sensitivity, spectral flexibility, and in some cases, imager response time. Recently invented is the Coded Access Optical Sensor (CAOS) Camera platform that works in unison with current Photo-Detector Array (PDA) technology to counter fundamental limitations of PDA-based imagers while providing high enough imaging spatial resolution and pixel counts. Using for example the Texas Instruments (TI) Digital Micromirror Device (DMD) to engineer the CAOS camera platform, ushered in is a paradigm change in advanced imager design, particularly for extreme dynamic range applications.

**Keywords:** Camera, Optical Imager, Imaging Device, Digital Micromirror Device.

## 1. INTRODUCTION

Imagine that you are driving at night. You are tired. Suddenly, you see a bright light approaching you, getting even brighter. It is the headlights from a truck. At that instant, human vision is impaired due to the dazzling brightness. You hope for the best that in the next few moments, the truck will pass you by without another vehicle appearing in or near your lane. Such wishful thinking on a statistical scale can be life threatening, so today the automobile industry is developing cameras for day and night vision to improve driving safety [1-2]. Even the United Nation (UN) has launched a global program called —“Decade of Action for Road Safety 2011–2020” to plan for improved safety global vehicle operation environments.

Today’s large-scale deployment multi-pixel CMOS (complementary metal-oxide-semiconductor) and CCD (charge-coupled devices) camera technology intrinsically supports 60 dB level linear dynamic ranges that can reach higher 100 dB level dynamic ranges using a variety of techniques, such as using hardware modifications in the sensor chip by increasing pixel size and pixel integration time or by using several pixel resets within the integration time to implement range compression before saturation and using photo-diode pixel response curves to decompress the optical irradiance data to the full range [3]. Another hardware approach uses a spatially varying exposure method by depositing neutral density filters on the pixel array so some pixels recover the brighter zones and others catch the weaker light areas [4]. Unlike linear CMOS/CCD/FPA sensors where pixel photo-voltage is proportional to the incident light irradiance on the pixel, an alternate design CMOS sensor has been implemented to achieve higher dynamic range by using per pixel logarithmic amplifiers to compress the photo-detected electrical signal (i.e., photo-voltage is a logarithm of the incident light irradiance), although at the cost of increased readout noise due to the limited voltage swing for the read-out electronics giving reduced sensitivity which leads to lower image contrasts [5]. Another approach called lin-log uses a linear response of the pixel over the lower dynamic range while a log response over the brighter region of the image [6]. This method maintains the better sensitivity (and image contrast) in the lower dynamic range region but produces lower sensitivity and signal-to-noise in the log compressed higher dynamic range (HDR) of the camera. In addition, software methods such as deployment of multi-image capture processing have been used to increase the dynamic range but at the cost of producing image combination artefacts with varying signal-to-noise ratio image capture [7]. Specifically, multi-image processing to produce an HDR image puts certain constraints of both the camera operation and viewed scene. For

instance, a small camera aperture creating a large depth of field is needed; plus the scene should have no motion and the camera should be on a tripod, otherwise one gets ghosting. In addition, the scene should not have a shallow depth of field as then the post-processing produces image artefacts. Do note that using a smaller aperture in the camera also leads to lower light levels on the optical sensor, adding further challenges for extreme dynamic range image capture and recovery.

For the vehicle safety application, efforts have started to deploy current multi-pixel sensor technology to design vehicle cameras. One such effort's simulations reached a 100 dB dynamic range for visible-Near Infrared camera. This camera by Sensata Technologies (USA) used a custom CMOS sensor design to implement 6 pixel resets within the integration time to implement multiple slopes-based range compression before saturation and used photo-diode pixel response curves to decompress the optical irradiance data to the full range [3]. Another approach from a French group used a commercial SONY global shutter 640 x 480 CCD 60 dB dynamic range sensor combined with circular exposure control of the sequential multiple captured frames and multi-frame image processing algorithm to improve the monochrome dynamic range of the vehicle camera over the standalone Sony CMOS sensor camera [7]. This camera on average took 80 seconds to register a high dynamic range image. It is also relevant to point out that recently Raptor Photonics (UK) announced a new visible-SWIR (400 nm to 1700 nm) camera [8]. This 1280 x 1024 pixel count with up-to 60 Hz frame rate camera is designed using a cooled InGaAs PIN Photo-Diode Array sensor with a 10 micron resolution. The camera is specified with a 70 dB dynamic range. Another recent announcement on the sensor chip level happened in September 2016 and is from Omnivision that introduced a 30 frames/second 94 dB single exposure linear dynamic range CMOS 2M pixels sensor chip OV2775, although restricted for the visible band [9]. This CMOS sensor has a dual exposure mode that increases the dynamic range to 120 dB. In addition, log CMOS sensors from New Imaging Technologies (NIT) indicate log response dynamic range of 140 dB [10] while Photonfocus provides lin-log CMOS sensors [11] with a 60 dB linear dynamic range and log response over the 60 dB to 120 dB range. Another CMOS sensor design called DR-Pix by Aptina (now ON-Semi) uses controlled on/off switching of a capacitor within each pixel circuit to allow two different, i.e., bright light and low light modes of operation. This CMOS sensor has a 82.9 dB dynamic range and a newer version has a maximum 96 dB dynamic range [12]. Clearly, these recent camera and CMOS chip developments indicate the commercial need and value with respect to high dynamic range cameras. Nevertheless, these CMOS sensor each have their fundamental limitations. Particularly, when using non-linear pixel responses that reduce signal-to-noise, sensitivity, color reproduction, and image contrast, creating non-uniform imaging quality.

Although today's commercial multi-pixel sensor-based imagers can have excellent spatial resolution and pixel count with improving dynamic ranges for the acquired visible band image, the camera is fundamentally designed from a mainly fixed space-time-frequency pixel view point where the image acquisition work load is placed equally on the large number (e.g., 1,000,000) of individual pixels (point photo-detectors) in the camera. In many applications, the light irradiance ( $W/m^2$ ) levels are not uniformly distributed across the image space with some pixel zones carrying extremely bright light irradiances and others with very weak light levels. This is counter intuitive to the equal work load assigned to all pixels in the classic and dominant multi-pixel image sensor design method. Specifically, multi-pixel photo-detection devices such as CCD/CMOS and Focal Plane Array (FPA) sensors have inherently small quantum well sizes that limit the camera performance in terms of pixel saturation levels, linearity, limited image read-out speed, blooming and spill-over caused inter-pixel crosstalk and inter-pixel dead zone light scattering. In addition, depending on the wavelength and type of FPA, cooling is required to produce low noise and higher dynamic range.

It is important to appreciate that fundamentally using current PDA technology, one simply collects imaged light in a continuous wave (or DC light) fashion with the bright pixel detection in the PDA device mainly constrained by the limited quantum full well capacity of the small and fixed active area of the photo-sensor pixel as well as by the bright photons generated shot noise in the pixel. In the case of imaged dim light detection with a current PDA device, the electrical dark current noise in the tiny fixed area pixel restricts the output electrical signal-to-noise ratio and thus the ability to decipher the dim light electrical signal from the detector noise floor. Thus, to expect a quantum jump in the dynamic range provided by a new camera technology, it is reasonable to assume that a paradigm change is required in camera design that avoids the continuous wave or DC light collection via a fixed active area pixel approach that provides a DC electrical signal output from the imager.

Thus, there exists a challenge to design, build, and test a smart extreme linear dynamic range wavelength band flexible camera where scenes exist with both bright and weak light targets of extreme importance that need adequately fast application dependent reliable detection to enhance safety of both human and machine operations. Again, it is important to stress that the desired camera should have the capability to provide extreme linear dynamic range adequate intelligent image pixel information fast enough for pattern recognition (e.g., like an identify friend or foe (IFF) decision

in military systems) to make a potentially lifesaving vehicle platform operator decision versus receiving an extreme megapixel count super high spatial resolution limited dynamic range image that fails to detect the targets of interest in the extreme contrast scene.

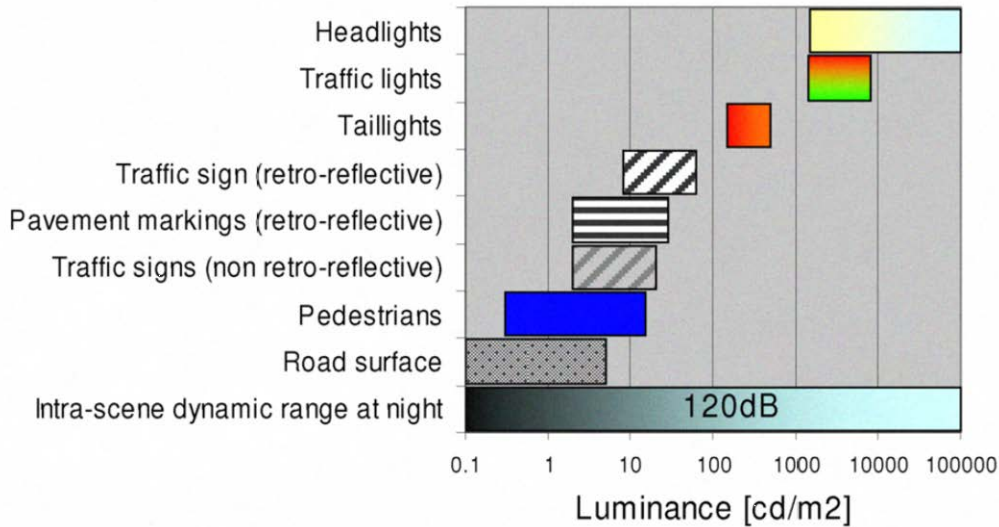


Fig. 1: Luminance ranges of traffic scenes at night [3].

Today, there still remains a challenge for cameras to reach extreme linear dynamic ranges of 190 dB with real-time multi-colour capture of extreme contrast images. For example as shown in Fig.1 using ref.3 data, at least a 120 dB intra-scene dynamic range is present in natural night scene settings facing the 2009 automobile environment. This intra-scene dynamic range requirement is even higher to prevent colour signal clipping for deciphering the fundamental red (R), green (G), and blue (B) colours to assemble a natural true colour image. Today, when considering additional light pollution with uncontrolled lighting around the globe, the natural night scene settings facing the current automobile environment is even more demanding dynamic range-wise. Although the vehicle scenario is a key motivation for developing an extreme dynamic range camera to enable greater human and transportation infrastructure safety, there are other man-made machine vision applications that also operate within extreme optical contrast environments. The common theme of these extreme contrast images and applications is that there are some critical image zones in the viewed scene that are extremely bright and other vital image zones that are extremely dark; hence the extreme dynamic range imager challenge where one needs to “see” both types of targets using the camera unit.

## 2. CAOS CAMERA – A NEW PARADIGM IN SMART CAMERA DESIGN

To take on the challenge of smart extreme contrast imaging such as for the vehicle environment, I recently invented the CAOS camera. CAOS stands for Coded Access Optical Sensor. The origins of the CAOS camera are inspired by a postgraduate course I took in 1985 at the California Institute of Technology (Caltech) with the late Physics Nobel Prize-winning Prof Dr Richard Feynman. I recall Prof Feynman basically saying: There is Radio Moscow in this room, there is Radio Beijing in this room, there is Radio Mexico city in this room; then he paused and said: aren't we humans fortunate that we can't sense all these signals; if we did we would surely go mad with the massive overload of electromagnetic radiation (radio signals) around us!

These words of wisdom have stayed with me for over 30 years and combined with my Caltech PhD Thesis work in 1987 in spinning optical disk distributed local oscillator RF signal spectrum processing [13] and my mid-90's interest in the DMD, all led to the CAOS invention. Specifically, all the radio signals that Professor Feynman mentioned do exist simultaneously in space, but each are carrying their unique signature or time-frequency domain radio code. Today, using advanced device and design technologies, even the weakest of these Radio Frequency (RF) signals can be detected using a sensitive enough RF receiver that is tuned to the specific radio code. This is indeed the basis of the world's wireless mobile phone network, so why not apply this RF wireless multiple access phone network design philosophy to the optical imaging scenario with multiple pixels of light?

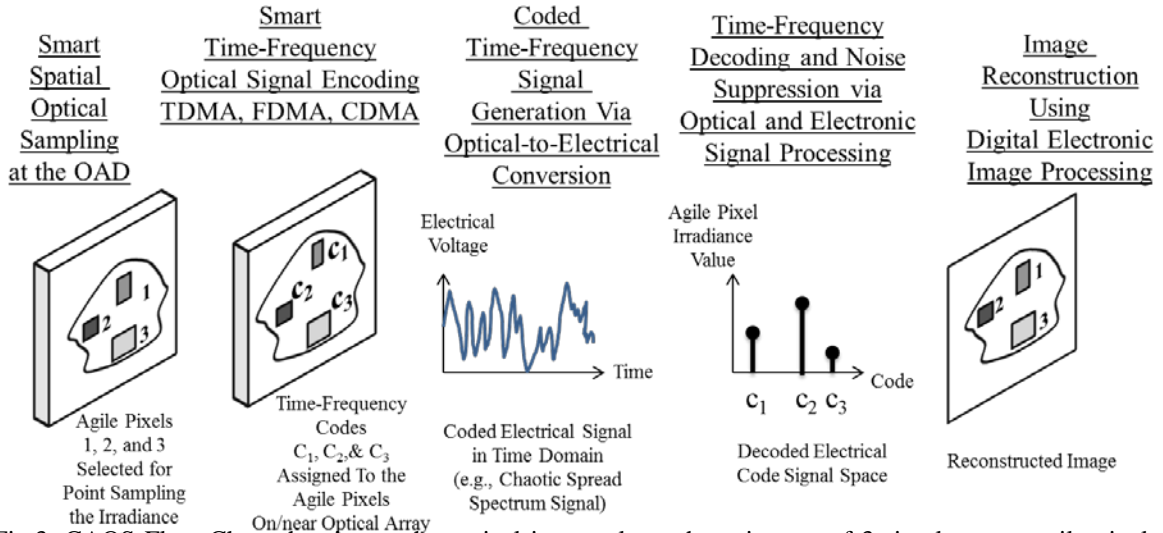


Fig.3. CAOS Flow Chart showing at the optical image plane, the existence of 3 simultaneous agile pixels of different sizes, locations, and shapes, each RF modulated with its own time-frequency code.

Thus, CAOS is born where agile pixels of the light selectively captured from an image space (see Fig.3) are rapidly encoded like RF signals in the time-frequency-space domain using an Optical Array Device (OAD) such as a multi-pixel spatial light modulator (SLM). RF coded light from these agile pixels is simultaneously detected by one point optical-to-RF detector/antenna. The output of this optical detector undergoes RF decoding via electronic wireless-style processing to recover the light levels for all the agile pixels in the image. On the contrary, CCD/CMOS cameras simply collect light from an image, so photons are collected in the sensor buckets/wells are transferred as electronic charge values (DC levels). There is no deployment of time-frequency content of the photons. CAOS forms an active imager when the OAD is a time-frequency-amplitude modulated light source array. Hence, CAOS forms both a passive and/or active imager and is a paradigm shift in imager design empowered by modern day advances in wireless and wired devices in the optical and electronic domains.

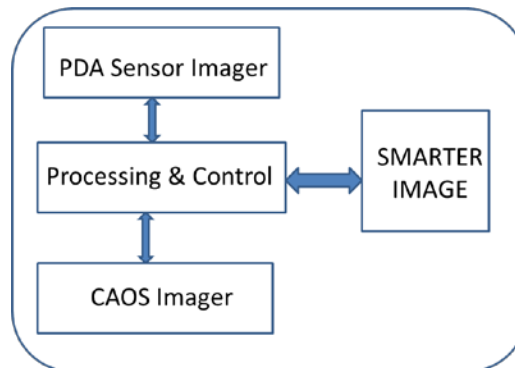


Figure 4: The CAOS Camera – A smart camera design combining CAOS and Photo-Detector Array (PDA) sensor (e.g., CMOS/CCD/FPA) technology.

Furthermore, the CAOS camera (see Fig.4) works in unison with current limited linear dynamic range multi-pixel sensors (e.g., CMOS/CCD/FPA) to smartly and simultaneously engage photonic as well as electronic signal processing in the CAOS-mode time-frequency coding domain to make possible an exceptional performance desired hybrid (H) imager. In effect, the PDA imager guides the selection of agile pixels in the CAOS imager to pull out image data from regions of interests where an extreme dynamic range enquiry is necessary for optimal imaging. CAOS breaks

the prior-art paradigm of equal work load for all pixels in the image zone by smartly creating agile pixels to match the pixel work load where it is most needed, in as sense, creating a distributed work load model to match the typical scene application. The hybrid nature of the CAOS camera also exists on the image processing level where the CAOS platform hardware is used to implement classic linear and non-linear imaging techniques (including via iterative algorithms) to quickly pull-out lower dynamic range estimates of the observed scene in order to guide the extreme dynamic range CAOS-mode operations of the camera. The CAOS camera also has the spectral flexibility as well as the extreme dynamic range to work both as an active (e.g., using laser illumination) or passive (using ambient light) camera. This is important given the trend to deploy eye safe lasers in vehicle vision systems in order to see under difficult imaging conditions. CAOS is inherently multidisciplinary as it leverages interplay of techniques and devices from the varied fields of RF/optical wireless and wired communications, RF (analog) and digital signal processing, RF radar, coding theory, optical displays, and photonic signal processing.

To put things in context, frequency coding of light dates back to 1949 when M. Golay [14] used rotating disk patterned grating-based frequency (Hz) coding of the spatially separated spectral components of light along with a single point photo-detector to design a high throughput and signal-to-noise ratio spectrometer and later in 1968, P. Gottlieb [15] independently applied the same coding concept using a scanning patterned reticle to design an imaging display. Independently, in 1987, N. A. Riza in his Caltech Ph.D. studies used a chirped patterned grating spinning optical disk to generate an optically spatially distributed local oscillator to implement RF spectrum analysis of an RF modulated light source [13]. In the late 1960s independently Ibbett [16] and Decker [17] suggested the spatial [not frequency (Hz) domain] coding of light for the design of higher signal-to-noise ratio spectrometers and Decker [18] also suggested its use for making an imager. Specifically in these designs, the  $N$  spatially separated light spectral channels (or image pixel channels) are multiplied by  $N$  different spatial 2-D orthogonal (matrix) masks, one mask at a time. For each of mask, the total light from all the  $N$  light channels is collected at one time by one point-PD to give an intensity reading. So for  $N$  different masks, one gets  $N$  independent intensity readings (DC values) that are stored sequentially and then later are subjected to inverse matrix (transform) processing to recover the incident light intensity of the  $N$  spectral/spatial channels. It is important to note that this method is a time sequential method that used spatial coding and is not the Golay-type frequency (Hz) coding of the spatially separated spectral data. Both Fellgett [19] and Gottlieb [15] had independently also pointed out the higher signal-to-noise ratio benefit of detecting many (e.g.,  $N$ ) simultaneous optical (spatial/spectral) channels (i.e., the multiplex advantage) by the point-PD versus using one at a time single pixel/wavelength channel detection using a time sequential light capture, e.g., done by moving a slit in time to implement an optical scanning spectrometer that is equivalent to producing  $N$  spectral slits.

Also note that the TI DMD SLM has been used with CCD/CMOS imagers for spectrometry [20] plus control of camera parameters such as blooming [21], Field of View (FOV) and pixel level irradiance integration times [22]. Motivated by extreme brightness spectrally diverse laser source imaging, the Riza group has proposed and demonstrated the agile pixel starring-mode DMD-based imager [23-25]. Such a DMD-based imager has also been used to implement compressive sensing that uses image spatial projection measurements with iterative image processing algorithms to recover the pseudorandom spatial code sampled original image [26]. Compressive sensing for imaging essentially assumes that the image has sparse spatial image content [27-29], implying that its spatial frequency content is mainly in the lower part of the spatial frequency spectrum, thus allowing under-sampling (below Nyquist limit) of the image scene. To put today's compressive sensing field in context, it is also important to note that since at least 1968, image compression using spatial transforms (e.g., Fourier and Hadamard [30] variety) and image recovery using inverse transforms of compressed frequency space data has been applied to enable systems with data bandwidth and processing overhead reduction.

In contrast, the imaging works described by the Riza group [23-25] and described here directly sample and preserve the true optical irradiances of the incident image and the fundamental CAOS-mode [31-35] extreme dynamic range multiple access imaging procedure is not based on classic compressive sensing techniques [29]. In compressive and transform sensing, spatial projections across the image spatial domain are in play for sparse sampling and the collected time sequential data is next subjected to iterative algorithm or inverse transformations (spatial correlations) with non-linear or linear processing, respectively. On the contrary, time-frequency content (Hz domain) of the selected simultaneous agile pixels in the image is in play via time-frequency correlations (transforms) for CAOS-mode camera image capture and recovery. In other words, spatial locations of the selected agile pixels with respect to each other have no fundamental role (e.g., via spatial correlations) in the individual pixel irradiance time-frequency encoding and decoding process implemented for CAOS-mode of the camera.

It is important to note that the spatial size, location and shape of each agile pixel in the smart pixel set that is sampling the incident image region of interest in the CAOS camera is smartly controlled using prior or real-time image

application intelligence gathered by the CAOS-mode imaging working in unison with other classic multi-pixel sensors as well as computational imaging methods operating within the CAOS hardware platform. Thus the proposed CAOS camera forms a Hybrid (H) design smart imaging platform. For example, limited dynamic range image intelligence can be quickly gathered using classic compressive sensing [27-29]. As mentioned, this computational technique is based on image spatial projections data combined with numerical optimization processing and will use the same CAOS hardware platform to give the estimated lower dynamic range image. In this hybrid design case, the CAOS camera agile pixel acquires a kind of space-time-frequency representation. Other linear transform computational methods [16-18, 30] can also be deployed within the CAOS camera platform by appropriately programming spatial masks on the SLM. Thus the proposed *CAOS camera platform is a true hybrid design, both from a hardware point-of-view as well as a computational point-of-view*, unleashing the strengths of various technologies and methods while countering their limitations to deliver the best image possible for the given application.

Given the time-frequency domain processing's tremendous time-bandwidth product (TBWP) using current wired and wireless optical (optoelectronic) and RF (electronic) technology, the CAOS camera is in the position to exploit this TBWP via high gain high noise suppression coherent Digital Signal Processing (DSP) to enable the desired smart camera for vehicle and other high contrast imaging applications. In addition, the point PD deployment in the H-CAOS camera provides the use of one (or possibly two) extremely large quantum well capacity bucket (s) (without potential temperature cooling) to collect time-frequency modulated light generated electronic charge from the selected simultaneous agile pixels on the image irradiance map. This leads to the extreme instantaneous dynamic range capability of the raw camera output signal that is further subjected to analog-to-digital conversion and smart DSP for further dynamic range enhancement. These mentioned feature form the core of the CAOS camera.

### 3. CAOS CAMERA DESIGNS AND DEMONSTRATIONS

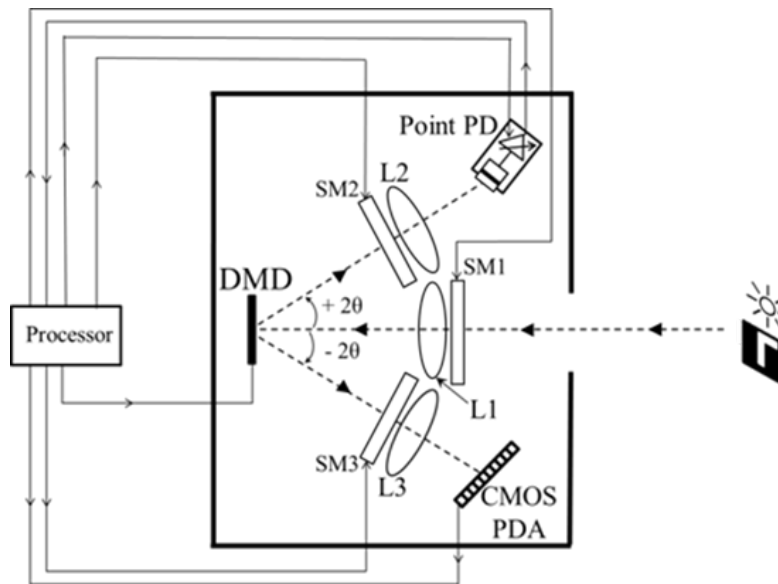


Figure 5: H-CAOS camera design using a DMD as the OAD and a CMOS PDA as the Hybrid (H) element. L1/L2/L3: Lenses. SM1/SM2/SM3: Smart Modules for light conditioning. PD: Photo-Detector with amplifier. [33]

A variety of CAOS-mode camera designs have been described by us [32]. For example, a version of the CAOS camera called the CAOS-CMOS camera (see Figure 5) has been recently built and demonstrated using the Texas Instruments (TI) DMD SLM as the CAOS-mode time-frequency agile pixel encoder [33]. The experiment used wireless Frequency Division Multiple Access (FDMA) style coding and decoding of the agile pixels with system operations details described in our recent Optics Express publication [32]. This visible band CAOS camera demonstrated a 30 dB improvement in camera dynamic range over a standard commercial 51 dB dynamic range CMOS camera when subjected

to three test targets that created a scene with extreme brightness as well as extreme contrast ( $> 82$  dB) High Dynamic Range (HDR) conditions.

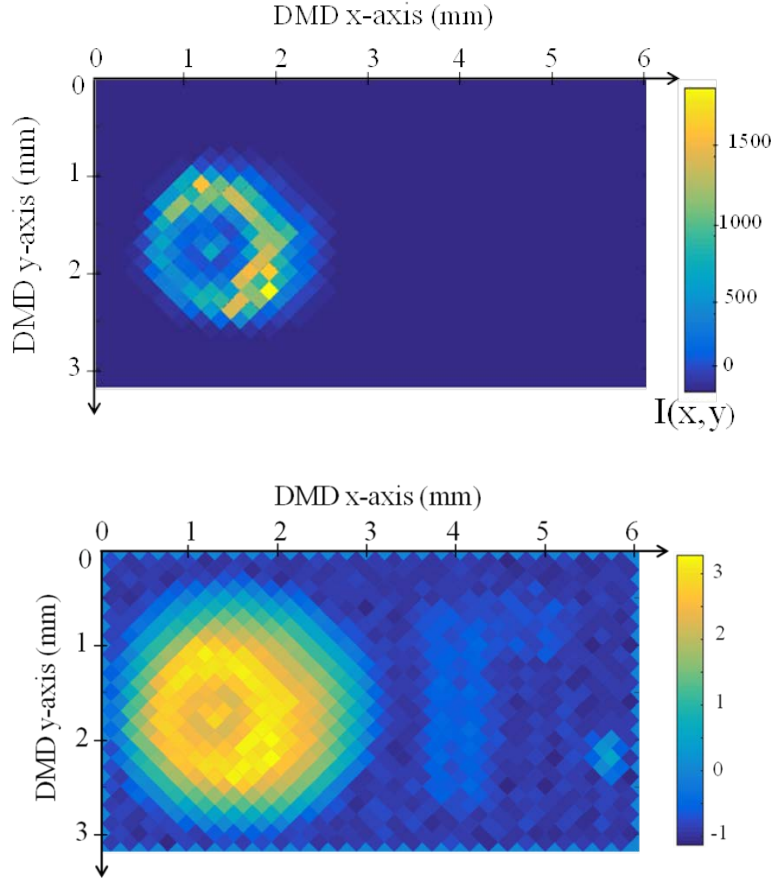


Figure 6. 82 dB HDR scaled irradiance map of the CAOS-mode acquired image in a linear (top photo: two faint targets not seen) scale and logarithmic (bottom photo: all three targets seen) scale. [33]

Specifically, as shown in Figure 6, this CAOS camera produced target on the left edge of the image is extremely bright while the two targets to the right of the bright target are extremely non-bright targets, near the noise floor of the demonstrated camera. Yet, the demonstrated CAOS camera is able to correctly see all three targets without using any attenuation of the incoming light from the imaged scene. Note that any attenuation of the light to eliminate saturation of the CMOS sensor sends the weak light images into the noise floor of the CMOS sensor, making it impossible to see the weak light targets. Note that the choice of the 51 dB CMOS camera and 82 dB target was chosen for the first incoherent light CAOS experiment to demonstrate the principle of the smart CAOS camera, i.e., when the CMOS sensor fails to detect targets in the scene, the CAOS-mode is deployed to sift the region of interest and recover a missing potential target. This was indeed achieved using the chosen hardware set-up.

Furthermore, for a first demonstration of the basics of the CAOS camera, we choose to image the 2-D irradiance map of a CW visible laser beam that showcases both extreme brightness and dim light zones [31]. The CAOS camera was set-up using a TI DMD (see Fig.7(d)). As shown in Fig.7, we generate the full image of the incident laser beam irradiance by operating the CAOS camera agile pixel in a hybrid FDMA plus TDMA mode by scanning 3 agile pixels in a raster format line scan and collecting the PD data for Fast Fourier-Transform (FFT) processing and agile pixel irradiance decoding. Three agile pixels at a time at the DMD chip plane are coded with on/off modulations of  $f_1 = 80.1$  Hz,  $f_2 = 133.4$  Hz, and  $f_3 = 200.2$  Hz resulting from the two-tilt state nature of the DMD chip micromirrors.

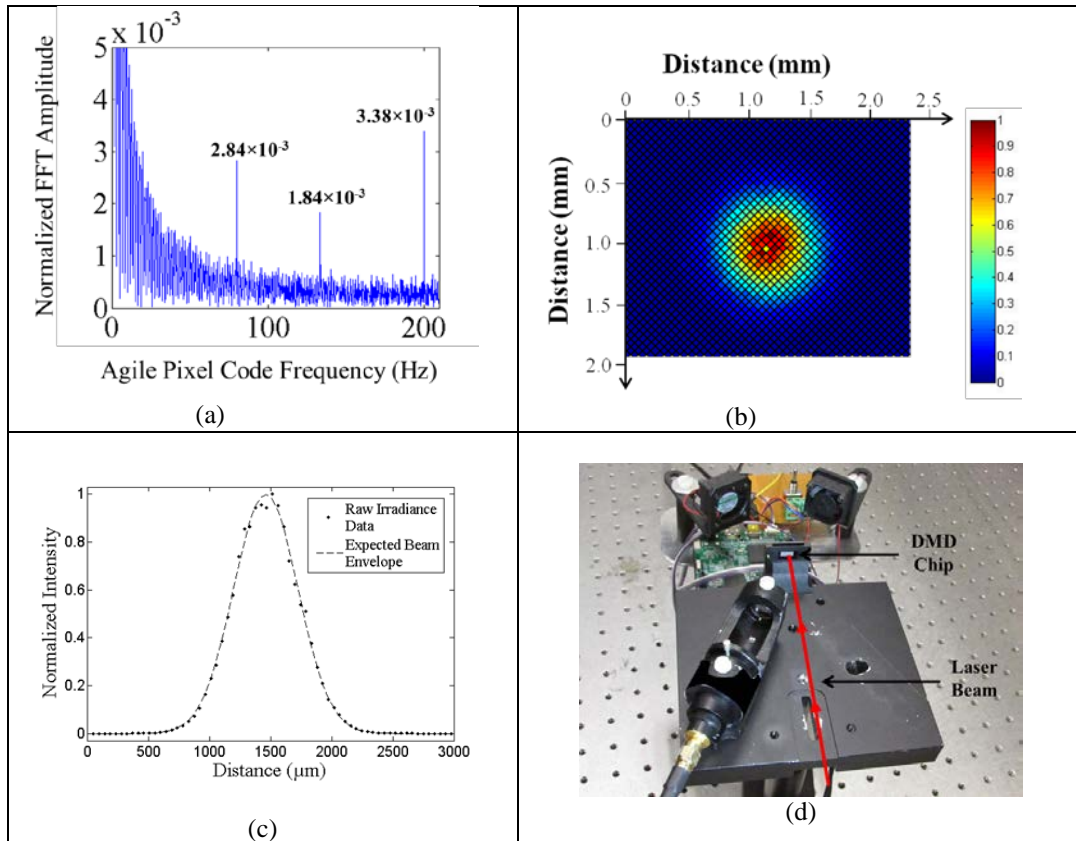


Fig.7(a) FFT signal processing decoding of the three micromirrors agile pixel irradiances  $I_1$ ,  $I_2$ , and  $I_3$  that are proportional to the normalized spectral values computed by the FFT operation. (b) shows the 2-D irradiance of 2160 agile pixels data ( $60 \times 36 = 2160$ ) from the experimental CAOS camera demonstrating a 77 dB dynamic range.(c) Comparison of central cross-section data of the CAOS camera acquired laser beam image (dots) vs. laser manufacturer provided theoretically expected Gaussian beam envelope (dashed line). (d) CAOS camera optical experimental setup [31].

Fig.7(a) shows the FFT signal processing decoding of the three agile pixel irradiances  $I_1$ ,  $I_2$ , and  $I_3$  at the DMD chip. To generate preliminary CAOS image data giving a 77 dB dynamic range, the imager operated with a total of 2160 agile pixels time modulating via FDMA coding in sets of three with each set modulating for 6.24 seconds followed by a 14 seconds delay before the next set modulated to ensure synchronisation between PC,  $\mu\text{C}$  and LCr DMD board with each agile pixel being  $6 \times 6$  micromirrors, with a micromirror with  $7.64 \mu\text{m}$  sides. Compared to our previous non-time coded starring mode DMD agile pixel imager [23], the dynamic range of the CAOS camera has improved by 5 orders of magnitude ( $>55$  dB). The manufacturer specified laser beam radius value is within 0.75% error (i.e.,  $100\% \times (529.9 - 526) / 529.9$ ) of the CAOS camera Fig.7(c) data provided 2-D Gaussian fitting measurement.

Depending on a vision system's broadband wavelength requirements suited to a particular night time application such as using targeted eye safe laser illumination (e.g., 860 nm, 1064 nm, 1550 nm) for active vision and imaging through fog, an alternate proposed dual-band CAOS vision system optical design such as shown in Fig.8 can be deployed [34-35]. This CAOS camera operates as a dual-band camera, e.g., Visible and NIR bands, giving an extreme dynamic range for both bands. Recall that Raptor Photonics (UK) introduced a new visible-SWIR (400 nm to 1700 nm) camera with a limited 70 dB dynamic range and a need for detector cooling [8]. CAOS dual-band camera design removes both these limitations.

The Fig.8 CAOS dual band design also features another special CAOS property, namely, the TF1/TF2 tunable optical filters can use a DMD or another SLM to implement the CAOS-mode for the image wavelengths of interest. Fig.9 shows a possible DMD TF design within the Fig.8 context indicating that a dual CAOS mode camera is realized for precision HDR color imaging.

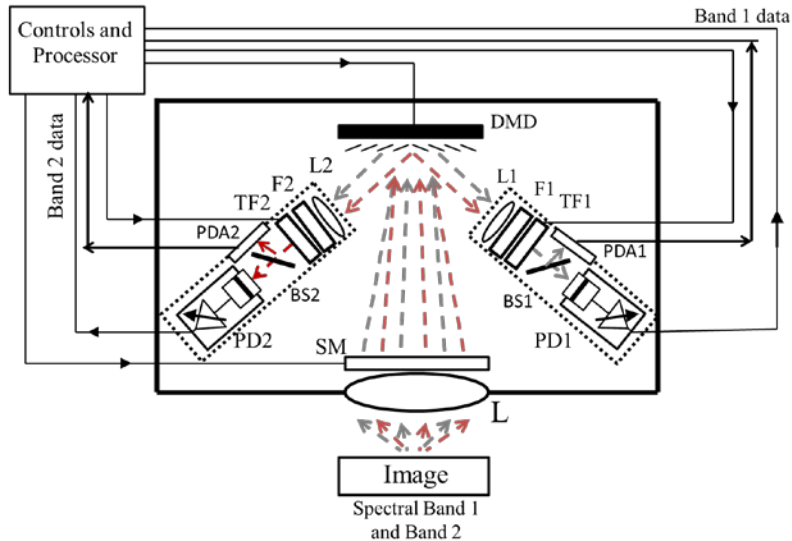


Fig.8. CAOS camera design for simultaneous dual-band imaging. F1/F2 are fixed broadband filters. TF1/TF2 are tunable optical filters. PDA1/PD2 are Photo-Detector Array Devices. BS1/BS2: Beam splitters. PD1/PD2: Point detectors. F1 allows band 1 passage and F2 allows band 2 passage [35].

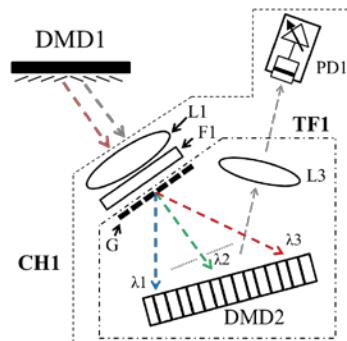


Fig.9 A possible DMD TF design for CAOS mode operations within the wavelength bands. G: Grating or wavelength dispersion element [35].

As mentioned earlier, the early CAOS camera demonstrations showed around 80 dB linear dynamic ranges for the camera. To improve on this result, we decided to use a controlled optical attenuation visible laser beam as a direct target incident on the agile pixel on the DMD plane of the CAOS camera. We controlled the optical attenuation over a 10 million to 1 ratio (or a 140 dB camera dynamic range). Using this test target set-up and improved electronic signal processing techniques, we were able to demonstrate a 136 dB linear dynamic range [35] for the CAOS camera and this is essentially a 40 dB improvement in linear dynamic range over a 2016 state-of-the-art linear CMOS sensor. Our dual-band CAOS camera also demonstrated a dual-band image with better than  $-60$  dB inter-band crosstalk when using a visible-SWIR test target made up of  $2 \times 2$  array of 3 visible and one SWIR LEDs (see Fig.10) [35].

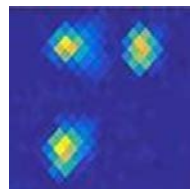


Fig.10. Visible band image captured by the Dual-band CAOS Camera using three visible LEDs and one SWIR LED target scene with LEDs arranged in a  $2 \times 2$  formation. The SWIR LED as expected is missing from the camera visible channel created image [35].

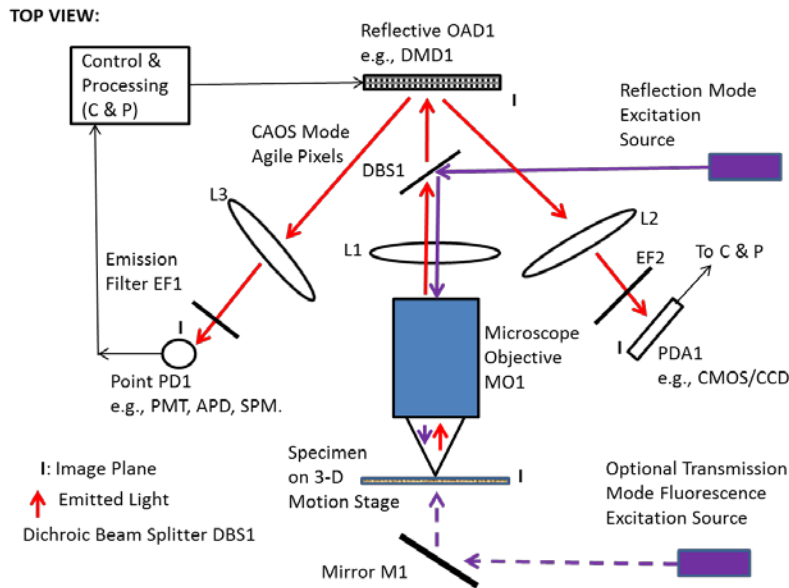


Fig.11. CAOS Smart Fluorescence Microscope/Nanoscope.

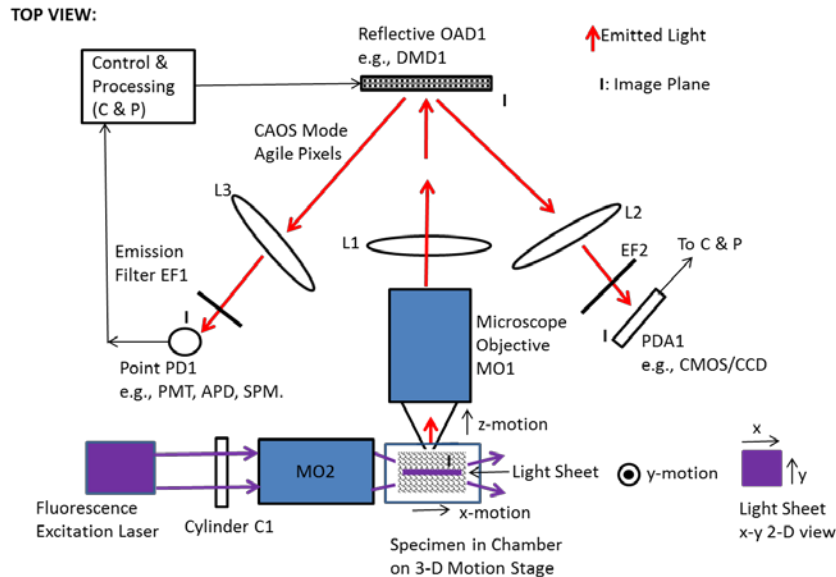


Fig.12. CAOS Smart Fluorescence Light Sheet Microscope/Nanoscope for 3-D Imaging.

The CAOS camera platform can also be configured to form optical microscopes and nanoscopes for both 2-D and 3-D imaging of biological and other specimens. Fluorescence microscopy and nanoscopy is a powerful tool in medical imaging and Fig.11 and Fig.12 show designs for a CAOS smart fluorescence microscope and a CAOS nanoscope. In both cases, designs are shown using a reflective OAD, e.g., a DMD. The transverse ( $x$ - $y$ ) resolution in the classic sense for both these designs is given by the OAD pixel size assuming the objective and tube lens ( $L1$ ) optics is diffraction limited. If each OAD pixel in the CAOS-mode T-F modulates a single fluorescence emission from a specimen spatial emission site that is smaller than the classic Abbe diffraction limit, then the CAOS microscope can function as a nanoscope as it has collected light from a nanoscale emitter. Coupled with 3-D nano-motion stages, a full 3-D nanoscale image is possible if controlled emissions are generated from the specimen. The Fig.12 design engages light sheet

microscopy to enable 3-D imaging with the CAOS platform, although other 3-D imaging designs such as confocal and wavelength multiplexed access are also possible. Note that again CAOS works in collaboration with the classic 2-D sensors (e.g., CCD, CMOS, etc) to extract the needed biological target information via CAOS-mode to enable extreme dynamic range low crosstalk imaging. Multiple CAOS-mode agile pixels can be simultaneously engaged by the user for efficient image data extraction. The Fig.11 and 12 designs also apply to traditional non-fluorescence microscopes. Fig.13. shows a proposed CAOS smart Digital Holography (DH) microscope using a Mach-Zehnder type interferometer design. DH produces high contrast interferograms where the CAOS-mode can be a powerful method to extract digital hologram data to assist the classic PDA DH sensor to enable smart DH-based imaging.

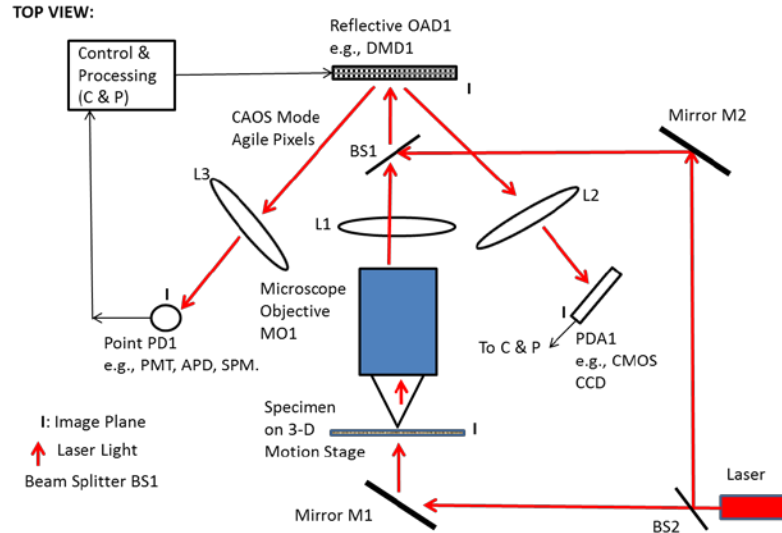


Fig.13. CAOS Smart Digital Holography Microscope.

#### 4. CAOS CAMERA ANALYSIS

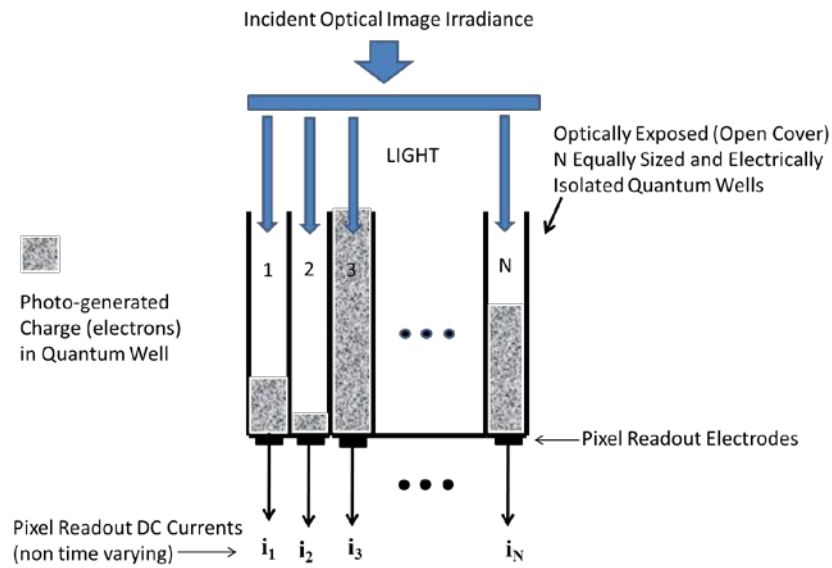


Fig.14. Operation of a classic PDA sensor (shown is side view of sensor).

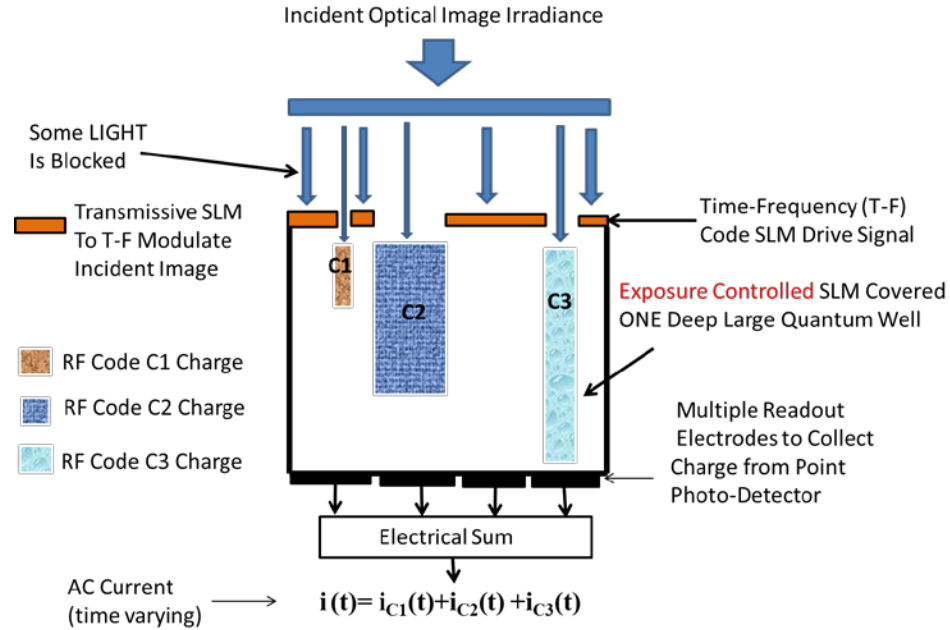


Fig.15. Basic operation of the point PD in the CAOS camera (shown is side view of sensor).

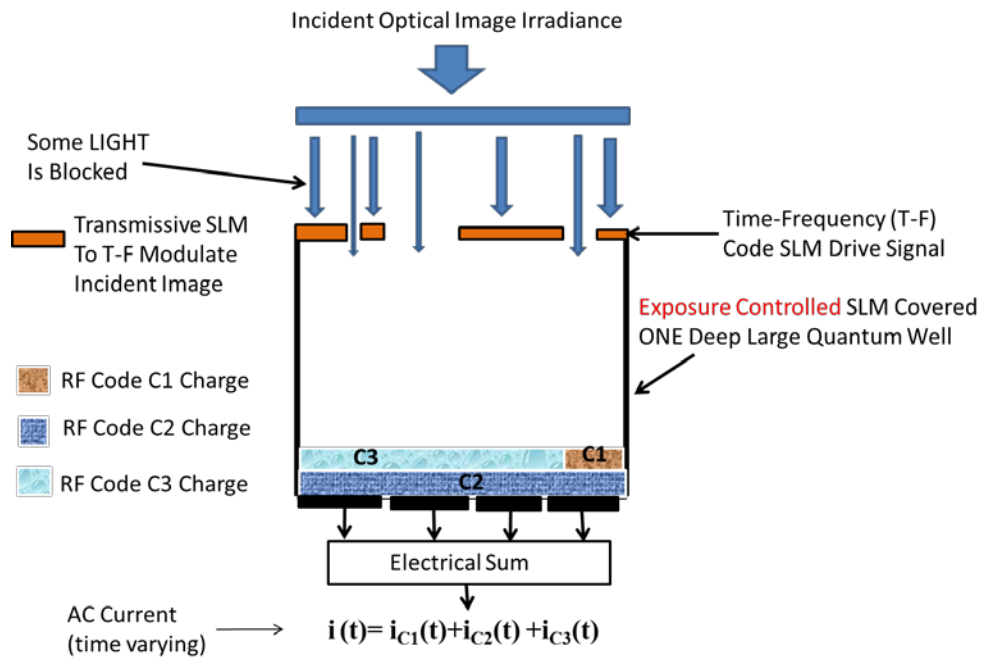


Fig.16 A more accurate illustration of Fig.14 showing how the 3 coded charge packets can fill the quantum bucket.

Fig.14. shows the operation of a classic PDA sensor made up of  $n=N$  equal sized and physically isolated and independently read pixels. Each  $n$ -th pixel produces a DC level current ( $i_n$ ) or voltage signal representing the photo-generated charge collected in the individual pixel quantum well for one frame charge integration time of the camera. 4 pixels are shown with photo-generated charge of various fill levels. Pixel 3 is saturated and causes charge spill over into adjacent pixels. Pixel 2 quantum well is mostly empty. All pixels are optically exposed to the incident light as there is no

physical cover preventing light from reaching the pixels. This is unlike the CAOS camera where selected light is blocked from reaching the point PD photo-sensitive zone. It is important to note that some area of the PDA sensor light striking zone is used up by the pixel electronic circuitry used to control and read charge from the individual pixels. So in general, a PDA has a lower fill factor (i.e., optically exposed area) when compared to a point PD of same quantum well physical dimensions. Fig.15. shows the basic operation of the point PD in the CAOS camera. The point PD shown is one large quantum well (e.g., same total charge capacity as the Fig.14 PDA sensor) that can have a multiple electrodes to read the total charge. The SLM produces an exposure controlled cover over the point PD with different sized openings corresponding to the chosen agile pixel sampling spatial resolutions. Each  $n$ -th opening (agile pixel) is time-frequency modulated with its time-frequency coded signal  $c_n(t)$  that in-turn time-frequency modulates the incident image light at this specific agile pixel location. This modulated light next creates a time-frequency code modulated photo-generated charge in the well that is collected at the PD output as a cumulative RF AC signal simultaneously representing all the  $n=N$  coded light regions of the incident image. In the figure, there are 3 independent T-F coded light regions representing 3 agile pixels in the CAOS camera. Much like a RF wireless signal produced by the mobile phone antenna, the AC signal provided by the photo-electrical transducer (point PD) is next subject to electronic conditioning and extreme dynamic range advanced signal processing for agile pixel irradiance (and spectral) decoding and image construction. The Fig.15 illustration shows the 3 independent coded photo-generated charge assemblies as different sized rectangles suspended in the quantum well cavity with the top sides of the rectangles matching the agile pixel openings in the deployed SLM encoder. In reality, the 3 coded charge distributions simply fill the same quantum bucket and are not physically separate in the bucket. Fig.16 shows a better illustration how the 3 coded charge packets fill the quantum bucket, making efficient use of the bucket capacity. Here the challenge to separate the 3 coded charge packets falls on the electronic post-processing that must have quality T-F codes to isolate the charged packets from each other for low agile pixel crosstalk image recovery.

In summary, it is important to point out that the CAOS camera inherently makes the best and most efficient use of the relatively large full quantum well capacity of the point detector used in the CAOS camera. Such is generally not the case in prior-art PDA-based cameras where an incident bright extreme contrast image causes the many high spatial resolution smaller capacity quantum wells to be partially filled while many other quantum wells in the PDA are over filled and create spill over to nearby wells, thus causing pixel saturation and inter-pixel crosstalk noise. The CAOS camera point PD can be filled with adequate light levels to provide the best signal-to-noise ratio for incident irradiance map decoding operations. In short, ***CAOS is also quantum well capacity efficient and signal-to-noise ratio optimizable.***

Electronics plays a major role in the CAOS camera. Electronics is both used for camera control as well as camera wireless type signal processing to extract Digital Signal Processing (DSP) gain noise suppression as well as to accomplish agile pixel irradiance encoding and decoding. Component control is implemented through a dedicated microcontroller while the signal processing system includes the chain of devices starting from the point PD(s) and their interface and gain electronics to the A-D converter and image processor that includes the agile pixels encoder and decoder. There are also electronic interfaces between the PDA sensor and the CAOS platform to enable the CAOS camera. Electronics also controls the DMDs in the system. There is significant literature on the design of electronic control and data acquisition and processing systems within the optics and photonics context [37-40]. An embedded system design is possible to build a robust and efficient CAOS smart camera system.

Coding theory is also fundamental to the selection of agile pixel codes used in the CAOS-modes, both on the spatial image plane and the spectral filtering plane. Extensive work in coding channels for wired and wireless electronic and optical systems [41-43] has been conducted and this can be leveraged and optimized for the CAOS-mode. Issues to keep in mind include the family of codes, their orthogonality properties, code length, inter-code crosstalk, code robustness via error correcting codes, mixed code options including analog/digital coding, the encoding and decoding signal processing overheads, speed and robustness.

Complete electronic programmability gives the CAOS smart camera powerful attributes both as a smart spatial and spectral sampler of irradiance maps and also for electronic processing to enable high performance encoding and decoding of the agile pixel/spectral irradiance map. Much like wireless and wired communication networks, the agile pixel can operate in different programmable time-frequency coding modes like FDMA, CDMA, and TDMA. CDMA and FDMA will produce spread spectrum RF signals from the PD while TDMA is the staring-mode operation of the CAOS camera, one agile pixel at a time producing a DC signal. For full impact of the CAOS camera, agile pixel codes should include CDMA, FDMA or mixed CDMA-FDMA codes that produce not only PD signals on a broad RF spectrum but also engage sophisticated Analog (A), Digital (D), and hybrid information coding techniques to provide isolation (e.g., minimum cross-correlation) and robustness amongst time-frequency codes used for OAD pixel coding.

*The speed of image acquisition* by the CAOS-mode is limited mainly by the current 32 KHz frame refresh rate of TI DMD technology. A basic design example using a 14-bit CDMA code per agile pixel used for a 1000 simultaneous agile pixel generation with one code length PD integration time plus 1 ms for data processing creates a 1.4375 ms image frame time or 695 frames/sec camera. Increasing the PD integration time by a factor of 10 to 4.375 ms (now has 10 full code lengths) plus adding the 10 ms processing time creates a 14.375 ms image frame rate or near 70 frames/s camera. Clearly, the CAOS camera can be designed to register real-time 60 frames/s video common to most vehicle environment applications. Furthermore, the CAOS camera can be designed for faster than real-time video rates. On the spatial resolution of the CAOS-mode acquired image, this resolution depends on the size of the agile pixel and can be as small as a single micromirror in the DMD. It is important to point out that other types of SLMs/OADs can also be used to build the CAOS camera, thus controlling camera features such as frame rates and spatial and spectral resolutions.

## 5. CONCLUSION\*

This paper has highlighted the CAOS smart camera that highlights a new paradigm in smart camera design where one combines the strengths of classic PDA sensors with the CAOS-mode of the CAOS smart camera to produce imaging features that are otherwise not possible using a PDA sensor-only design. The CAOS-mode works in collaboration with and not in competition with the PDA sensor forming a hybrid design and operations camera. Intelligence for the CAOS-mode of the smart camera comes by engaging both the unique CAOS camera provided hardware, as well as by executing classic and newer computational imaging methods within this overall hardware (including the PDA sensor). Such an approach smartly delivers the best image possible for the user such as creating an extreme (e.g., 190 dB) linear dynamic range agile pixel target in a critical scene with deeply hidden targets that are otherwise unseen using classic PDA sensors. Presented are designs of a fluorescence CAOS microscope and a fluorescence CAOS light sheet microscope for 2-D and 3-D imaging, respectively. A CAOS microscope design is also shown for implementing smart DH. It is important to note that like any new imaging platform technology, true realization of the CAOS camera's full strengths is challenging and requires careful and focussed research and development matched to the critical application needs.

\* Additional information on the CAOS camera including videos, papers is available at [www.nabeelriza.com](http://www.nabeelriza.com).

## REFERENCES

1. Decade of Action for Road Safety (2011–2020): Global Launch, World Health Organization (WHO), Geneva.
2. A. Mukhtar, L. Xia, and T. B. Tang, "Vehicle Detection Techniques for Collision Avoidance Systems: A Review," *IEEE Transactions on Intelligent Transportation Systems*, Vol. 16, no. 5, October 2015.
3. D. Hertel, H. Marechal, D. A. Tefera, W. Fan, and R. Hicks, "A low-cost VIS-NIR true color night vision video system based on a wide dynamic range CMOS imager," *IEEE Conf. Intelligent Vehicles*, 2009.
4. Toshiba TCM5117PL CMOS Image Sensor data sheet, 2013.
5. Y. Ni and K. Matou, "A CMOS log image sensor with on-chip FPN compensation," in *Proc. 27th Eur. Solid-State Circuits Conf.*, pp. 101–104, Sep. 2001.
6. G. Storm, R. Henderson, J. E. D. Hurwitz, D. Renshaw, K. Findlater, and M. Purcell, "Extended dynamic range from a combined linear-logarithmic CMOS image sensor," *IEEE J. Solid-State Circuits*, 41, 9, pp.2095-2106, 2006.
7. Y. Li, Y. Qiao, and Y. Ruichek, "Multiframe-Based High Dynamic Range Monocular Vision System for Advanced Driver Assistance Systems," *IEEE Sensors Journal*, Vol. 15, No. 10, October 2015.
8. Raptor Photonics's new OWL 1280 VIS-SWIR HD format camera press release, Oct.28, 2016.
9. Omnivision's new OV2775 CMOS 2M pixels sensor chip press release, Sept.19, 2016.
10. New Imaging Technologies (NIT), France, Native WDR log CMOS sensors brochure as of 2016 ([www.new-imaging-technologies.com](http://www.new-imaging-technologies.com)), brochure dated 2014.
11. Photonfocus AG, Switzerland, Lin-Log CMOS HD1-D1312-160-CL data sheet ([www.photonfocus.com](http://www.photonfocus.com)) 2016.
12. Aptina DR-Pix technology CMOS sensor, Aptina Imaging Corporation 2010 white paper (now ON-Semi), and ON-Semi AR0237CS CMOS sensor data sheet with max 96 dB dynamic range, 2016.
13. N. A. Riza, Chapter 4: Optical Disk-based Acousto-Optic Spectrum Analysis, Caltech Ph.D. Thesis, Oct. 1989. Also presented in N. A. Riza et.al, *OSA Annual Mtg paper*, Vol.15, 1990.
14. M. J. E. Golay, "Multi-slit spectrometry," *J. Opt. Soc. Am.* 39(6), 437-444 (1949).
15. P. Gottlieb, "A television scanning scheme for a detector-noise limited system," *IEEE Trans. Inform. Theory* 14(3), 428-433 (1968).

16. R. N. Ibbett, D. Aspinall, and J. F. Grainger, "Real-Time Multiplexing of Dispersed Spectra in Any Wavelength Region," *Applied Optics*, Vol. 7, No. 6, pp. 1089-1093, June 1968. (received Nov.13, 1967)
17. J. A. Decker, Jr. and Martin O. Harwitt, "Sequential Encoding with Multislit Spectrometers," *Applied Optics*, Vol. 7, No. 11, pp. 2205-2209, November 1968. (received June 13, 1968)
18. J. A. Decker, Jr., "Hadamard-Transform Image Scanning," *Applied Optics*, Vol. 9, No. 6, 1392-1395, June 1970.
19. P. Fellgett, "I.—les principes généraux des méthodes nouvelles en spectroscopie interférentielle-A propos de la théorie du spectromètre interférentiel multiplex," *J. phys. radium* 19, no. 3, 187-191, 1958.
20. K. Kearney, and Z. Ninkov, "Characterization of a digital micro-mirror device for use as an optical mask in imaging and spectroscopy," *Proc. SPIE* 3292, 81 (1998).
21. J. Castracane, and M. Gutin, "DMD-based bloom control for intensified imaging systems," *Proc. SPIE* 3633, 234 (1999).
22. S. Nayar, V. Branzoi, and T. Boulton, "Programmable imaging using a digital micro-mirror array," *Proc. of IEEE Conf. on Computer Vision and Pattern Recognition* 1, 436-443 (2004).
23. S. Sumriddetchkajorn and N. A. Riza, "Micro-electro-mechanical system-based digitally controlled optical beam profiler," *Appl. Opt.*, 41(18), 3506-3510 (2002).
24. N. A. Riza and M. J. Mughal, "Optical Power Independent Optical Beam Profiler," *Opt. Eng.*, 43(4), 793-797 (2004).
25. N. A. Riza, S. A. Reza, and P. J. Marraccini, "Digital micro-mirror device-based broadband optical image sensor for robust imaging applications," *Opt. Commun.*, 284(1), 103-111 (2011).
26. D. Takhar, J. N. Laska, M. B. Wakin, M. F. Duarte, D. Baron, S. Sarvotham, K. F. Kelly, and R. G. Baraniuk, "A New Compressive Imaging Camera Architecture using Optical-Domain Compression," *Proc. SPIE* 6065, 606509 (2006).
27. E. Candès, J. Romberg and T. Tao, "Robust uncertainty principles: exact signal reconstruction from highly incomplete frequency information," *IEEE Trans. Inf. Theory*, Vol. 52, pp. 489-509, 2006.
28. E. Candès and J. Romberg, "Sparsity and incoherence in compressive sampling," *Inverse Problems*, IOP Publishing, Vol. 23.3, p.969, 2007.
29. J. Romberg, "Imaging via compressive sampling [introduction to compressive sampling and recovery via convex programming]," *IEEE Signal Processing Magazine*, Vol 25.2, pp. 14-20, 2008.
30. W. K. Pratt, J. Kane, and H. C. Andrews, "Hadamard transform image coding," *Proceedings of the IEEE*, Vol. 57, No.1, pp.58-68, 1969.
31. N. A. Riza, M. J. Amin and J. P. La Torre, "Coded Access Optical Sensor (CAOS) Imager," *Elsevier Journal of the Eur. Opt. Soc. Rap. Pub. (JEOS:RP)*, 10(15021), (2015).
32. N. A. Riza, "Coded Access Optical Sensor (CAOS) imager and applications," *SPIE Photonics Europe Conf. Proc., on Optics, Photonics and Digital Technologies for Imaging Applications*, Vol, 9896, paper No.9, Brussels, April 2016.
33. N. A. Riza, J. P. La Torre, and M. J. Amin, "CAOS-CMOS camera," *Opt. Express*, 24(12), 13444-13458 (2016).
34. N. A. Riza, and J. P. La Torre, "CAOS-CMOS multispectral and hyperspectral camera," *OSA Congress on Light, Energy and the Environment, Topical Meeting: Hyperspectral Imaging and Sounding of the Environment (HISE)*, Proc. Paper, Germany (2016).
35. N. A. Riza and J. P. La Torre, "Demonstration of 136 dB dynamic range capability for a simultaneous dual optical band CAOS Camera," *Optics Express*, Vol.24, Dec.12, 2016.
36. H.-S. Lee, C. G. Sodini, K. G. Fife, "Precise MOS imager transfer function control for expanded dynamic range imaging," *U.S. Patent* 6,600,471, July 29, 2003.
37. C. Laperle and M. O'Sullivan, "Advances in high-speed DACs, ADCs, and DSP for optical coherent transceivers," *IEEE/OSA J. Lightw. Technol* 32.4, 629-643, 2014.
38. P. J. Winzer, "Scaling Optical fiber networks: challenges and solutions," *OSA OPN Magazine*, 26, no. 3, 28-35, March 2015
39. T. H. Wilmshurst, "Signal recovery from noise in electronic instrumentation," Second Edition, CRC Press, 1990.
40. M. Johnson, "Photodetection and measurement: Maximizing performance in optical systems," (McGraw-Hill, 2003).
41. W.C.Y. Lee, "Mobile Communication Design Fundamentals", John Wiley and Sons, New York, (1993).
42. N. Karafolas and D. Uttamchandani, "Optical fiber code division multiple access networks: A review," *Optical Fiber Technology*, 2.2 149-168 (1996).
43. T. Richardson and R. Urbanke, "Modern coding theory," (Cambridge University Press, 2008).